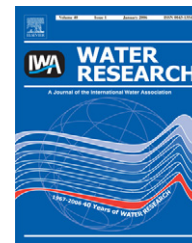


Available at www.sciencedirect.comjournal homepage: www.elsevier.com/locate/watres

Propham mineralization in aqueous medium by anodic oxidation using boron-doped diamond anode: Influence of experimental parameters on degradation kinetics and mineralization efficiency

Ali Özcan^a, Yücel Şahin^{a,*}, A. Savaş Koparal^b, Mehmet A. Oturan^c

^aDepartment of Chemistry, Faculty of Science, Anadolu University, 26470 Eskişehir, Turkey

^bDepartment of Environmental Engineering, Faculty of Engineering and Architecture, Anadolu University, 26470 Eskişehir, Turkey

^cLaboratoire Géomatériaux et Géologie de l'Ingénieur, Université Paris Est, 5 bd Descartes, Champs-sur-Marne, 77454 Marne la Vallée Cedex 2, France

ARTICLE INFO

Article history:

Received 21 January 2008

Received in revised form

24 February 2008

Accepted 27 February 2008

Available online 4 March 2008

Keywords:

Propham

BDD anode

EAOPs

Hydroxyl radical

Degradation

ABSTRACT

This study aims the removal of a carbamate herbicide, propham, from aqueous solution by direct electrochemical advanced oxidation process using a boron-doped diamond (BDD) anode. This electrode produces large quantities of hydroxyl radicals from oxidation of water, which leads to the oxidative degradation of propham up to its total mineralization. Effect of operational parameters such as current, temperature, pH and supporting electrolyte on the degradation and mineralization rate was studied. The applied current and temperature exert a prominent effect on the total organic carbon (TOC) removal rate of the solutions. The mineralization of propham can be performed at any pH value between 3 and 11 without any loss in oxidation efficiency. The propham decay and its overall mineralization reaction follows a pseudo-first-order kinetics. The apparent rate constant value of propham oxidation was determined as $4.8 \times 10^{-4} \text{ s}^{-1}$ at 100 mA and 35 °C in the presence of 50 mM Na_2SO_4 in acidic media (pH: 3). A general mineralization sequence was proposed considering the identified oxidation intermediates.

© 2008 Elsevier Ltd. All rights reserved.

1. Introduction

It is well known that a lot of wastes are formed during the production of pesticides and their application processes (Felsot et al., 2003). Most of these compounds pose environmental problems due to their eco-toxicity and stability. The aqueous effluents contaminated by these pollutants must thus be treated before their injection in the natural environ-

ment. There are various methods for the treatment of these wastes such as activated carbon adsorption, chemical oxidation, biological treatment, etc. (WHO, 2001). But these classical processes are not generally sufficiently efficient in the elimination of these pollutants. For example, activated carbon adsorption involves phase transfer of pollutants without decomposition and thus induces another pollution problem. Chemical oxidation is unable to mineralize the

*Corresponding author. Tel.: +90 222 3350580x5786; fax: +90 222 3204910.

E-mail address: ysahin@anadolu.edu.tr (Y. Şahin).

Abbreviations: BDD, boron-doped diamond; AOPs, advanced oxidation processes; EAOPs, electrochemical advanced oxidation processes; MCE, mineralization current efficiency; HPLC, high-performance liquid chromatography; GC-MS, gas chromatography-mass spectrometry; LC-MS, liquid chromatography-mass spectrometry; IC, ion chromatography; UV, ultraviolet; TOC, total organic carbon; TC, total carbon; BA, benzoic acid.

0043-1354/\$ - see front matter © 2008 Elsevier Ltd. All rights reserved.

doi:10.1016/j.watres.2008.02.027

persistent organic pollutants. Concerning the biological treatment, the main drawbacks are non-efficiency in presence of non-biodegradable and toxic pollutants, slow reaction rates, disposal of sludge and the need for strict control of proper pH and temperature. In order to overcome these disadvantages, more powerful oxidation methods are required than those currently applied in wastewater treatments for achieving their complete destruction.

The development of new technologies such as advanced oxidation processes (AOPs) has attracted great attention during the last two decades for the treatment of toxic and persistent organic pollutants in aqueous media because of their ability to reach the total mineralization (Neyens and Bayeans, 2003; Pignatello et al., 2006; Oturan and Brillas, 2007). These processes involve chemical, photochemical or electrochemical techniques to bring about chemical degradation of organic pollutants. Among them, electrochemical advanced oxidation processes (EAOPs) offer many advantages such as low operational cost and high mineralization efficiency of pollutants compared to other known chemical and photochemical ones (Oturan, 2000; Oturan et al., 2001; Boye et al., 2002; Brillas et al., 2004; Diagne et al., 2007; Ozcan et al., 2007; Sirés et al., 2007). In this sense, anodic oxidation is a very common EAOP. In this process pollutants can be oxidized by direct electron transfer reaction from organics to the electrode surface or the action of highly oxidizing radical species (i.e. hydroxyl radicals) formed on the high O₂-overtoltage anode surface. In this manner, a wide variety of electrode materials such as dimensionally stable anodes (RuO₂ or IrO₂-coated Ti) (Simond et al., 1997), thin film oxide anodes (PbO₂, SnO₂) (Belhadj Tahar and Savall, 1998; Malpass et al., 2006), noble metals (platinum) (Vlyssides et al., 2004) and carbon-based anodes (Lissens et al., 2003) have been investigated. On the other hand, these electrodes have some drawbacks in the electrochemical oxidation of pollutants. The usage of the boron-doped diamond (BDD) as anode material in wastewater treatment processes has attracted great attention recently because of its high stability and efficiency (Guinea et al., 2008; Chen and Chen, 2006; Brillas et al., 2005; Un et al., 2007). This electrode allows the in-situ production of hydroxyl radicals from water (Eq. (1)) or hydroxide ion (Eq. (2)) oxidation on the electrode surface at large quantities (Comminellis, 1994; Marselli et al., 2003; Michaud et al., 2003; Canizares et al., 2004; Flox et al., 2005; Sirés et al., 2007). These radicals are very powerful oxidizing agents and they react unselectively with organics giving dehydrogenated or hydroxylated by-products until their total conversion into CO₂, water and inorganic ions:



or hydroxide ion at pH ≥ 10:



Propham is a carbamate herbicide for the control of weeds in alfalfa, clover, flax, lettuces, afflow, spinach, sugar beets and peas. It prevents cell division and acts on meristematic tissues. Moreover, it is an acetylcholinesterase inhibitor and at the same time it could be degraded into aniline metabolites that are more dangerous than the parent molecule (Orejuela and Silva, 2004). Therefore, the removal of propham from

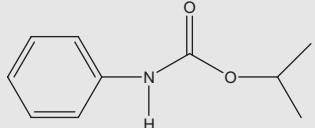
aqueous solution was performed previously by using the membrane separation technique (Kosutic and Kunst, 2002). Moreover, degradation of propham was investigated by using TiO₂ as heterogeneous photocatalyst (Muneer et al., 2005; Bahnemann et al., 2007). To the best of our knowledge, there is no study on the electrochemical oxidation of propham by anodic oxidation with a BDD anode. In this study, we examined the removal of propham from its aqueous solution by electrochemical oxidation using a BDD anode for the first time in the literature. The effects of important operating parameters such as applied current, temperature, pH and types of the supporting electrolyte on the degradation rate and mineralization efficiency were investigated. The oxidation by-products such as aromatics, short-chain carboxylic acids and inorganic ions were determined by high-performance liquid chromatography (HPLC), liquid chromatography–mass spectrometry (LC–MS), gas chromatography–mass spectrometry (GC–MS) and ion chromatography (IC) methods. Finally, an oxidative degradation pathway of propham by $\cdot\text{OH}$ radicals generated on BDD anode in aqueous medium was proposed.

2. Materials and methods

2.1. Chemicals

Propham was obtained from Riedel-de Haën. Its physicochemical properties are given in Table 1. Sodium sulphate (anhydrous, 99%, Across), sodium nitrate (99%, Merck), lithium perchlorate (99.99%, Aldrich), sodium chloride (99.7%, Merck) and potassium sulphate (99%, Fluka) were used as supporting electrolytes. Sulphuric acid (ACS reagent grade, Across), potassium hydrogen phthalate (Nacalai Tesque Inc.), hydrochloric (37%), perchloric, nitric and acetic acids (glacial p.a., Across) were obtained as reagent grade. Sodium nitrate and ammonium nitrate (99%, Merck) were used as standard solutions for the IC analyses. Sodium hydroxide and methanesulphonic acid and tetrabutylammonium hydroxide solutions were used as eluent and regenerant, respectively. Oxalic, maleic, glyoxylic, acetic, formic and

Table 1 – Physicochemical properties of propham

Chemical name	Isopropyl carbanilate
Chemical structure	
Molecular weight	179.2 g mol ⁻¹
Water solubility	32–250 mg L ⁻¹ at 20–25 °C
Melting point	87–88 °C
Adsorption coefficient, K(oc) ^a	1.604

^a K(oc) = (conc. adsorbed/conc. dissolved)/% organic carbon in soil.

oxamic acids were obtained from Fluka and used without further purification. All solutions were prepared by using pre-distilled $18\text{M}\Omega\text{cm}^{-1}$ deionized water (Sartorius).

2.2. Electrochemical cell

Experiments were performed in a 0.175 L undivided and thermostated cylindrical glass cell (5 cm diameter) equipped with two electrodes. The anode was a BDD thin film deposited on both sides of a niobium substrate ($3 \times 4\text{ cm}$) obtained from Magneto Chem. The cathode was Pt gauze (Aldrich). The distance between the electrodes was 3 cm. Before the degradation experiments, the electrode surface was cleaned in the propham-free solution by using the same conditions. The degradation experiments were performed by using aqueous solutions of propham (0.50 mM , 0.15 L^{-1}). In order to investigate the effect of the supporting electrolyte on the degradation of propham, one of the following salts was used in each experiment: Na_2SO_4 (0.05 M), NaNO_3 (0.1 M), NaCl (0.1 M) and LiClO_4 (0.1 M). The supporting electrolyte was 0.05 M K_2SO_4 in the by-products analysis. Prior to electrolysis, the pH of the solution was set to a known value: 3, 6, 9 and 11. Electrolyses were performed at current controlled conditions by using a constant current value (30, 50, 100, 300 and 500 mA). During the electrolysis, the reaction medium was agitated continuously by a magnetic stirrer (500 rpm) and samples were withdrawn from the reaction medium at regular time intervals.

2.3. Analytical procedures

The degradation of propham was monitored by HPLC using an Agilent 1100 system equipped with a diode array detector, an autosampler and a reversed-phase Inertsil ODS-3 ($5\ \mu\text{m}$, $4.6 \times 250\text{ mm}$) column. The column was thermostated at 40°C . Injection volume was $20\ \mu\text{L}$. The column was eluted with a mixture of water–methanol–acetic acid at 44:54:2 (v/v/v) with a flow rate of $0.9\text{ mL}\cdot\text{min}^{-1}$. Detection was performed at 254 and 280 nm. The aromatic intermediates were identified by retention time comparison and internal standard addition methods. Short-chain carboxylic acids were identified and quantified by a Supelcogel H column ($\phi = 7.8 \times 300\text{ mm}$). H_2SO_4 (4 mM) was used as mobile phase with a flow rate of $0.50\text{ mL}\cdot\text{min}^{-1}$. Detection was performed at 210 nm.

The concentrations of ammonium and nitrate ions released during the electrolyses were determined by IC (Dionex-100 equipped with a conductivity detector). A cation (IonPac[®] CS12A-Dionex) and an anion exchanger column (IonPac[®] AS14-Dionex) were used for ammonium and nitrate ion analyses, respectively. The injection volume was $25\ \mu\text{L}$. The mobile phase and regenerant were 20.0 mM methanesulphonic acid and 100.0 mM tetrabutylammonium hydroxide solutions for the cationic column, respectively, with a flow rate of $0.85\text{ mL}\cdot\text{min}^{-1}$. On the other hand, 30.0 mM sodium hydroxide and 22.0 mM H_2SO_4 were used for the anionic column as mobile phase and regenerant, respectively, with a flow rate of $0.80\text{ mL}\cdot\text{min}^{-1}$. Calibration curves were obtained by using the pure standards of the related ions.

The degradation of propham and its oxidation intermediates were monitored by LC–MS using an Agilent 1100 LC coupled to an Agilent 6300 mass spectrometer with an electron spray ionization interface and a heated nebulizer, in the positive mode. A reversed-phase Inertsil ODS-3 ($3\ \mu\text{m}$, $4.6 \times 150\text{ mm}$) column was used in the LC–MS experiments. The column was thermostated at 40°C . A volume of $20\ \mu\text{L}$ of sample was injected. The column was eluted with a mixture of water–methanol–acetic acid at 54:44:2 (v/v/v) with a flow rate of $0.5\text{ mL}\cdot\text{min}^{-1}$.

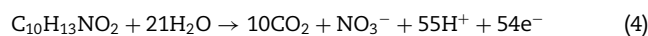
Some intermediates were identified by GC–MS (Thermo Finnigan PolarisQ GC–MS analyser). The treated solutions were extracted three times with dichloromethane and ethyl acetate and analysed by using a 25 m (i.d. 0.32 mm) SE-54 column. The temperature of the column was programmed. The initial temperature was 50°C for 2 min and increased up to 280°C with a rate of $10^\circ\text{C}\cdot\text{min}^{-1}$.

The total organic carbon (TOC) of the samples was determined by using a Shimadzu TOC-V analyser. The platinum catalyst was used in the combustion reaction. The carrier gas was oxygen with a flow rate of $150\text{ mL}\cdot\text{min}^{-1}$. The detector of the TOC system was a non-dispersive infrared detector. Calibration of the analyser was achieved with potassium hydrogen phthalate (99.5%, Merck) and sodium hydrogen carbonate (99.7%, Riedel-de Haën) standard solutions for total carbon (TC) and inorganic carbon (IC), respectively. The difference between TC and IC gives the TOC value of the sample.

The mineralization current efficiency (MCE) values were determined according to the following expression (Eq. (3)) (Hanna et al., 2005):

$$\text{MCE} = \frac{\Delta(\text{TOC})_{\text{exp}}}{\Delta(\text{TOC})_{\text{theor}}} \times 100 \quad (3)$$

where $\Delta(\text{TOC})_{\text{exp}}$ is the experimental TOC at a given time and $\Delta(\text{TOC})_{\text{theor}}$ is the theoretical TOC removal considering that applied electrical charge (= current \times time) is consumed for the mineralization of propham according to the electrochemical oxidation reaction (Eq. (4)), which presupposes the consumption of 54 F per mole of propham:



3. Results and discussion

3.1. Effect of applied current

The oxidation of organics on the BDD anode occurs by two ways: direct electron transfer from organics to BDD anode and oxidation by $\cdot\text{OH}$ formed on the BDD anode surface according to Eqs. (1) and/or (2) (Comminellis, 1994; Marselli et al., 2003). The latter process is more efficient in the degradation of organics on the BDD anode. The concentration of $\cdot\text{OH}$ radical depends on the applied current value. Therefore, here, the effect of applied current values on the degradation rate of propham was examined by using the applied current values of 30, 50, 100, 150, 300 and 500 mA. The obtained results are shown in Fig. 1. When the applied current

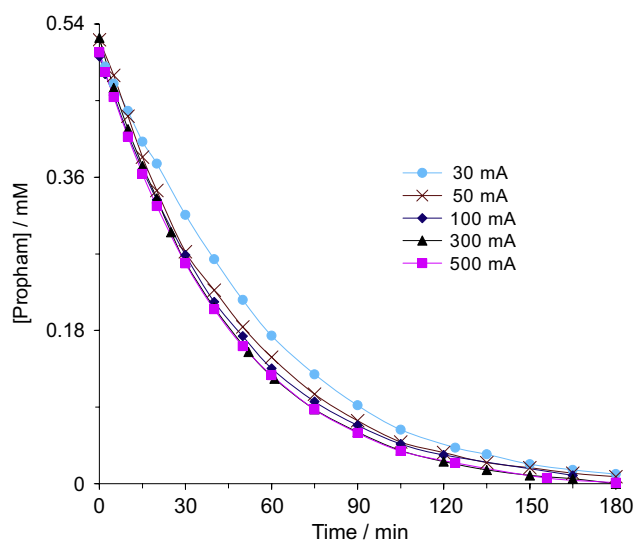


Fig. 1 – Effect of applied current on the propham degradation kinetics during the electrochemical oxidation using a BDD anode at room temperature: (●) 30 mA; (×) 50 mA; (◆) 100 mA; (▲) 300 mA; (■) 500 mA. [Propham]₀ = 0.5 mM, [Na₂SO₄] = 50 mM, pH: 3, V = 0.15 L.

value increased from 30 to 50 mA, a slight increase was observed in the degradation rate of propham. Beyond this value, the effect of applied current is not significant. In all cases, the degradation of propham was completed within 180 min. After this time, the main organics present in the solution are aromatic by-products and short-chain carboxylic acids. In order to clarify the oxidation ability of the system, we performed TOC analyses of the samples after 180 min of electrolyses (Table 2a) and corresponding MCE% values were calculated according to Eq. (3). As can be seen from Table 2a, the TOC removal values were increased and the MCE% values were decreased by increasing applied current. This decrease can be related to (i) the formation of O₂, which is more dominant than ·OH at high current (at voltage) values and (ii) the possible formation of weak oxidants as persulphate (Eq. (5)) and hydrogen peroxide.

It was interesting to note that while the initial degradation rate of propham was almost the same for all applied current values, the TOC removal values greatly increased at higher applied current values. This situation can be explained in the following way. The aromatic reaction intermediates formed by the oxidation of propham are more reactive towards hydroxyl radicals than propham. By increasing applied current values, the formation rate of ·OH also increased and these radicals were consumed simultaneously by the aromatic and aliphatic by-products. As a result the degradation rate of propham did not change significantly. On the other hand, the TOC removal values remained almost constant at 300 and 500 mA. The results show that the optimal current value was about 300 mA for the mineralization of propham. This result is in agreement with the literature (Panizza and Cerisola, 2005; Chen and Chen, 2006) because the oxidation of H₂O to O₂ is favoured in detriment of ·OH formation at high current values.

Table 2 – Effect of (a) applied current, (b) temperature and (c) supporting electrolyte on TOC analyses results and corresponding MCE% values for the anodic oxidation of propham after 180 min electrolyses time

	TOC (mg CL ⁻¹) ^{a,b}	TOC removal (mg CL ⁻¹) ^{a,b}	MCE ^{a,b,c} (%)
(a) Applied current (mA)			
30	24.12	38.65	77.68
50	14.31	48.46	58.44
100	10.16	52.61	31.72
300	3.48	59.28	11.92
500	3.12	59.64	7.2
(b) Temperature (°C)			
15	15.40	47.37	28.56
20	13.75	49.02	29.56
25	10.16	52.61	31.72
30	9.53	53.24	32.10
35	8.22	54.54	32.89
(c) Supporting electrolyte			
Na ₂ SO ₄	8.22	54.54	32.89
NaNO ₃	35.88	26.89	16.22
LiClO ₄	11.23	51.54	31.08
NaCl	19.39	43.38	26.16

Other operating conditions are given in Figs. 1(a), 2(b) and 4(c).
^a Initial TOC: 62.77 mg CL⁻¹.
^b Electrolysis time: 180 min.
^c Mineralization current efficiency values calculated from Eq. (3).

3.2. Effect of temperature

The effect of temperature on the anodic oxidation behaviour of propham was investigated at different temperature values between 15 and 35 °C at 100 mA constant current. The maximal value before the significant loss of water by evaporation is 35 °C (Boye et al., 2002). As can be seen from Fig. 2, the degradation of propham showed a similar trend for all temperature values. By increasing the temperature from 15 to 35 °C, a significant increase was obtained in the degradation rate of propham. TOC analyses were also performed for each trial and results are depicted in Table 2b. The initial TOC value of propham solutions (62.77 mg CL⁻¹) decreased to 15.40 and 8.22 mg CL⁻¹ for 15 and 35 °C, respectively, at the end of the 180 min electrolyses. The MCE% values also increased by increasing the temperature, which causes the improvement of the propham degradation rate. These results showed that TOC removal values were significantly enhanced by increasing the solution temperature. Similar results were previously reported by Sharifan and Kirk (1986) and Belhadj Tahar and Savall (1998). It can be explained in the following ways: (i) decrease of polymeric products formed during the oxidation process, (ii) increase of mass transfer rate of organics from solution to the electrode surface (Chen and Chen, 2006) and (iii) decrease of organics' stability as the reaction temperature increases.

3.3. Effect of pH

The pH of electrolyses medium is the other important parameter for the electrochemical oxidation procedures.

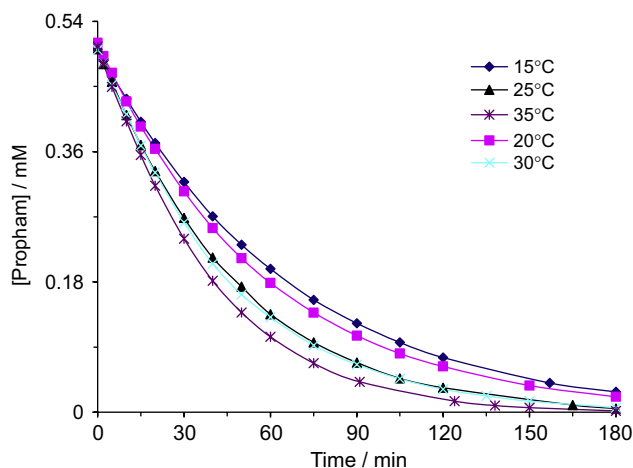


Fig. 2 – The effect of temperature on the degradation behaviours of propham by electrochemical oxidation on a BDD anode at 100 mA. (◆) 15 °C; (■) 20 °C; (▲) 25 °C; (×) 30 °C; (✱) 35 °C. [Propham]₀ = 0.5 mM, [Na₂SO₄] = 50 mM, pH: 3, V = 0.15 L.

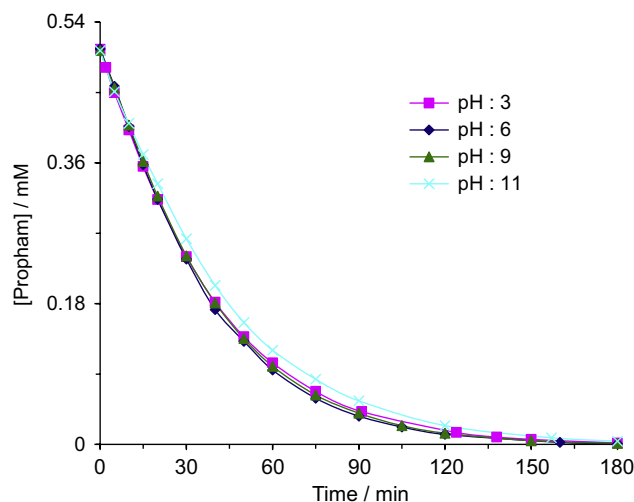


Fig. 3 – The degradation behaviors of aqueous solution of propham at pH values 3 (■), 6 (◆), 9 (▲) and 11 (×) by electrochemical oxidation on a BDD anode. [Propham]₀: 0.5 mM, [Na₂SO₄]: 50 mM, I: 100 mA, V: 0.15 L, T: 35 °C.

The effect of pH on the electrochemical oxidation of organics has been previously investigated by many authors (Canizares et al., 2004; Mitadera et al., 2004; Brillas et al., 2005; Flox et al., 2005; Martinez-Huitle et al., 2005; Polcaro et al., 2005; Muruganathan et al., 2007). Lissens et al. (2003) and Canizares et al. (2004) reported that the oxidation process is more favourable in alkaline media. In contrast, Martines-Huitle et al. (2007) and Scialdone et al. (2007) indicated that the efficiency of the process was increased in acidic media. According to this literature, it can be concluded that the effect of pH strongly depends on the nature of the investigated organics. Therefore, the effect of pH on the degradation rate of propham was studied at large pH range from acidic to basic. Aqueous solutions of propham (0.5 mM) were electrolysed at pH values of 3, 6, 9 and 11 (Fig. 3). As can be seen from this figure, the pH of the medium slightly affects the degradation kinetics of propham. A very small decrease was observed in the degradation rate at pH 11. This situation indicates that the degradation of propham can be performed at any pH value between 3 and 11 without any significant loss in oxidation efficiency of the system. There is no significant difference for the calculated TOC removal ($55 \pm 1 \text{ mg CL}^{-1}$) and MCE% ($\approx 33\%$) values at different pH values.

3.4. Effect of supporting electrolyte type

In order to verify the influence of the supporting electrolyte on the degradation kinetics and mineralization efficiency of propham aqueous solutions, the experiments were performed in acidic medium (pH 3) containing different supporting electrolytes as 0.05 M Na₂SO₄, 0.1 M NaNO₃, LiClO₄ and NaCl (Fig. 4). The degradation rate of propham was slightly increased when Na₂SO₄ was used as the supporting electrolyte instead of NaNO₃. As can be seen from Fig. 4, the complete degradation of propham almost took place in a 180 min electrolysis period in the presence of Na₂SO₄, NaNO₃ and LiClO₄. However, it finished in 15 min in the case of NaCl.

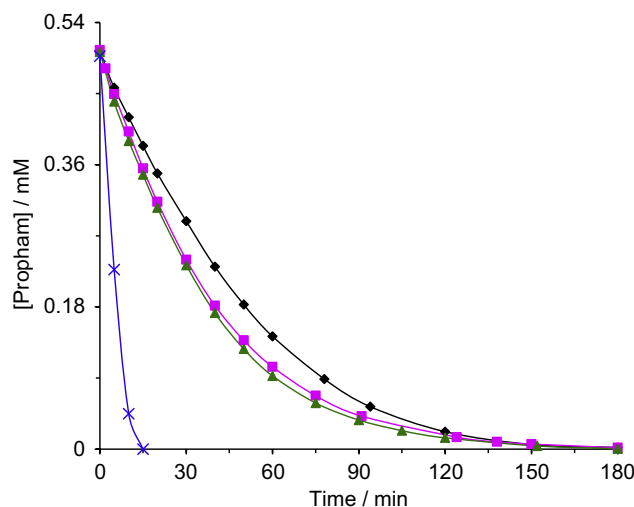
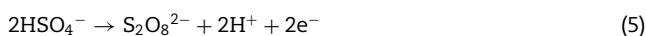


Fig. 4 – The effect of supporting electrolyte on the degradation behaviors of propham by electrochemical oxidation on a BDD anode: (▲) 0.05 M Na₂SO₄; (◆) 0.1 M NaNO₃; (■) 0.1 M LiClO₄; (×) 0.1 M NaCl. [Propham]₀ = 0.5 mM, I = 100 mA, V = 0.15 L, pH = 3, T = 35 °C.

In order to compare the TOC removal values of these systems, we performed the TOC analyses at 180 min electrolyses and calculated the corresponding MCE% values (Table 2c). The TOC removal and MCE% values of propham mineralization were increased in the following order: NaCl < NaNO₃ < LiClO₄ < Na₂SO₄. Although the use of NaCl as a supporting electrolyte has a very important effect on the propham degradation kinetics, this effect was not seen on the mineralization efficiency. These results can be explained in the following way: The SO₄²⁻ ions are easily oxidized at BDD anode to form persulphate (Eq. (5)) ions (Rodrigo et al., 2001; Panizza and Cerisola, 2005). These very reactive species can

also react with the organics and cause an increase the mineralization rate. The very fast degradation kinetics in the case of NaCl can be explained by a parallel degradation reaction in the solution phase via indirectly formed reactive species. The chloride ions were oxidized to chlorine gas (Cl_2) at the BDD anode (Eq. (6)), which reacts with water to form hypochlorite (ClO^-) ions (Eq. (7)) (Tatapudi and Fenton, 1994; Iniesta et al., 2001):



The formed chlorine gas, a strong chlorination agent, and hypochlorite ions can react with propham to form chlorinated by-products (Iniesta et al., 2001). The initial propham degradation kinetics enhanced and led to the formation of chlorinated by-products. As a result the mineralization efficiency and MCE% of propham aqueous solutions decreased.

3.5. Degradation and mineralization kinetics of propham

The degradation and mineralization kinetics of propham was investigated by electrolysing 0.5 mM propham aqueous solution at acidic media containing 0.05 M Na_2SO_4 at 100 mA constant current. The degradation kinetics of propham was followed by HPLC while the solution TOC removal as a mineralization measure was conducted by TOC analysis (Fig. 5). The propham concentration and TOC value of solution decreased with increasing electrolyses time, and complete degradation and mineralization were achieved in 180 and 480 min, respectively. The degradation of organics with

hydroxyl radicals generally follows the pseudo-first-order reaction kinetics in EAOPs (Guinea et al., 2008; Diagne et al., 2007; Oturan et al., 2001; Brillas et al., 2003). Therefore, the pseudo-first-order kinetic equation was used in order to determine the degradation and mineralization behaviour of propham. The obtained results were very well fitted to the corresponding straight lines (Fig. 5 inset). We thus calculated the apparent rate constant value (k_{app}) for the degradation of propham as $4.8 \times 10^{-4} \text{ s}^{-1}$ ($R^2: 0.9952$). The obtained results for the mineralization procedure showed two distinct straight lines. This situation can be explained in the following way. The dominant organic compounds in solution were short-chain carboxylic acids in the second step (after 180 min) because propham and its aromatic by-products were completely destructed during the first step as can be seen from Fig. 6a. The short-chain carboxylic acids are more resistant to mineralization by $\cdot\text{OH}$ (Buxton et al., 1988). Therefore, the mineralization rate of propham and the corresponding k_{app} value was decreased at treatment time up to 180 min.

3.6. Identification and evolution of degradation by-products

The oxidation of propham on BDD anode has led to the formation of aromatic by-products, short-chain carboxylic acids and inorganic ions. The identification of aromatic by-products obtained from the degradation of 0.5 mM propham aqueous solutions containing 0.05 M Na_2SO_4 at 100 mA constant current and pH 3 were performed by HPLC, GC-MS and LC-MS systems. The reversed-phase HPLC chromatograms showed that propham was converted mainly to a degradation by-product at the retention time of 6.16 min and to several other by-products at very low concentration levels. Some of them were identified as hydroquinone, benzoquinone and catechol with retention times of 3.36, 4.10 and 4.36 min, respectively. On the other hand, the GC-MS analyses results indicated that propham oxidation leads to the formation of two isomer products at the retention times of 9.32 and 9.97 min. According to molecular ion (M^+) and mass fragmentation, these by-products were identified as mono-hydroxylated forms of propham. The formation of these by-products can be explained as the *o*- and *p*-hydroxylation of benzene ring in propham structure (*o*- and *p*-hydroxyphenyl carbamic acid isopropyl ester). The LC-MS analyses of the same samples confirmed the formation of these two isomers at the retention time values 14.80 and 37.10 min. According to the polarities of the *o*- and *p*-hydroxyphenyl carbamic acid isopropyl ester, we thought that the by-product observed at 6.16 min in HPLC analyses should be the *p*-hydroxyphenyl carbamic acid isopropyl ester. The identified aromatic by-products and their evolutions are given in Table 3 and Fig. 6a, respectively. As can be seen in Fig. 6a, the only dominant aromatic by-product is *p*-hydroxyphenyl carbamic acid isopropyl ester as indicated before. While the concentration of propham was rapidly decreased during the oxidation process, those of the by-products were increased in the first 50 min of electrolyses. Finally, propham was completely converted to more simple products. The formation of benzoquinone was very fast and it reached its maximum concentration value at about 10 min and completely disappeared in 30 min. The

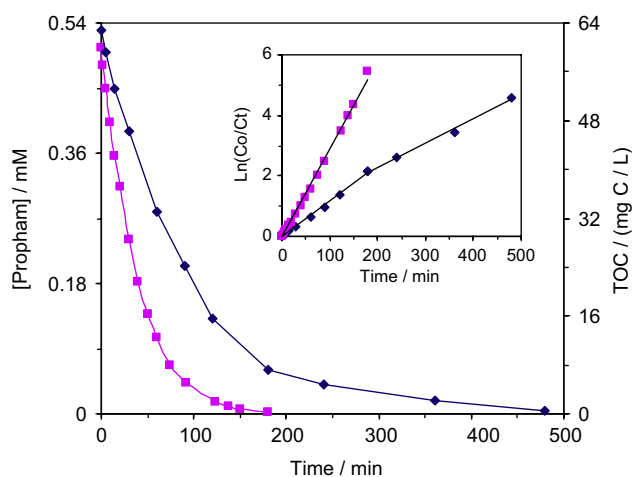


Fig. 5 – Kinetics behaviour of (■) 0.5 mM propham and (◆) solution TOC decay as a function of electrolyses time in aqueous solution during anodic oxidation with BDD anode. Inset shows the corresponding pseudo-first-order kinetics plots for (■) propham oxidation and (◆) mineralization kinetics. $I = 100 \text{ mA}$, $[\text{Na}_2\text{SO}_4] = 50 \text{ mM}$, $\text{pH} = 3$, $V = 0.15 \text{ L}$, $T = 35 \text{ }^\circ\text{C}$.

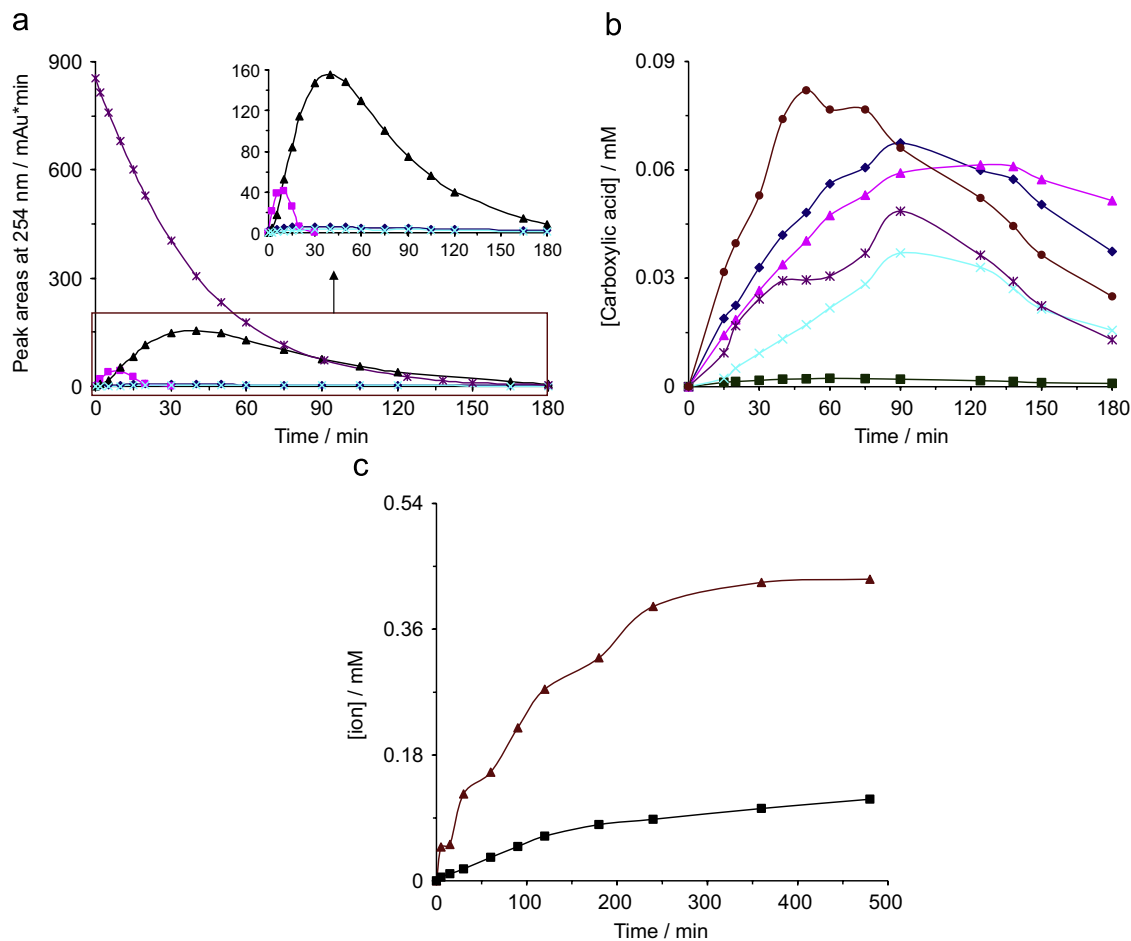


Fig. 6 – Time-course of the identified (a) aromatic by-products: (⋈) propham; (◆) hydroquinone; (■) benzoquinone; (▲) *p*-hydroxypropham; (×) *o*-hydroxypropham; (●) catechol, (b) short-chain carboxylic acids: (◆) oxalic; (■) maleic; (▲) oxamic; (×) glyoxylic; (⋈) formic; (●) acetic and (c) inorganic ions: (▲) NH_4^+ ; (■) NO_3^- during the anodic oxidation of 0.5 mM propham aqueous solution with BDD anode, $[\text{K}_2\text{SO}_4] = 50 \text{ mM}$, $I = 100 \text{ mA}$, $V = 0.15 \text{ L}$, $T = 35^\circ \text{C}$. The evolutions of by-products were determined by HPLC (a, b) and IC (c).

other aromatic by-products hydroquinone, catechol and *o*-hydroxyphenyl carbamic acid isopropyl ester concentrations remained at very small steady-state values during the electrolyses.

Ion-exclusion chromatograms of the above solutions showed the formation of several carboxylic acids as oxalic, maleic, oxamic, glyoxylic, formic and acetic acids with the corresponding retention times of 7.04, 8.91, 10.60, 12.37, 16.81 and 18.04 min, respectively. The evolution of these carboxylic acids during the anodic oxidation process is given in Fig. 6b. They are formed at high formation rates at the initial stage of the electrolyses, and they reached their maximal accumulation values in 90 min and then their concentrations were gradually decreased.

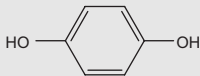
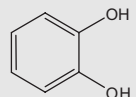
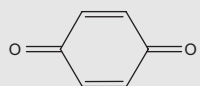
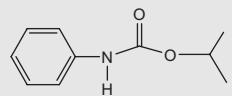
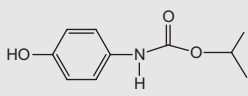
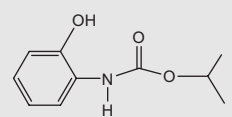
The identification and quantitative analyses of inorganic ions resulting from the mineralization of propham were performed by ion-exchange chromatography. The nitrogen atom present in the propham structure was converted to NO_3^- and NH_4^+ ions during the mineralization process. The evolution of these ions were given in Fig. 6c. As can be seen, ammonium ion concentration was gradually increased and it reached a steady-state value after 4 h. The formation rate of

nitrate ions during the degradation process was significantly slower than that of ammonium ion. This situation can be attributed to the electrochemical oxidation of NH_4^+ to NO_3^- and NO_2^- at BDD anode (Ammar et al., 2007). At the end of the electrolyses, the total concentrations of the ammonium and nitrate ions reached the stoichiometric ratio of the initial nitrogen. Almost 99% of the initial nitrogen was quantified after 8 h of treatment.

3.7. Mineralization pathway

The determination of the degradation by-products allows us to propose a mineralization pathway for the anodic oxidation of propham (Fig. 7). Electrogenerated hydroxyl radical was stated as BDD(OH) and for the sake of simplicity we gave the hydroxyl radical only at the beginning of the reaction sequence. The mineralization of propham mainly followed two parallel ways. Firstly, the mineralization started with hydroxylation of the electron-rich benzene ring of propham. $\cdot\text{OH}$ can be bounded preferentially to *ortho* and *para* positions. The formation of these two isomers, *p*-hydroxypropham and *o*-hydroxypropham, was observed during the experiments.

Table 3 – Identified aromatic by-products formed during the anodic oxidation of propham with BDD using LC–MS, HPLC and GC–MS systems

Chemical name	Chemical structure	Retention time	Mass fragmentation
Hydroquinone		3.31 ^a	–
Catechol		4.36 ^a	–
<i>p</i> -Benzoquinone		4.10 ^a	–
Propham (phenylcarbamic acid isopropyl ester)		13.36 ^a	–
<i>p</i> -Hydroxyphenyl carbamic acid isopropyl ester		8.22 ^b	179.1 (M ⁺), 137, 120.1, 93.1, 78.1, 66.1
		51.9 ^c	180.5 (M+1), 138.4, 120.4
		6.16 ^a	–
<i>o</i> -Hydroxyphenyl carbamic acid isopropyl ester		9.97 ^b	195.1 (M ⁺), 153, 136.1, 109.1, 91.1, 80.1, 52
		14.80 ^c	197.1 (M+1), 186.3, 154.4, 136.3
		10.51 ^a	–
		9.32 ^b	195 (M ⁺), 177.6, 153, 135.1, 109.1, 80.1, 52
		37.10 ^c	196.7 (M+1), 154.4, 121.3, 110.4

[Na₂SO₄] = 0.05 M, I: 100 mA, pH: 3, V = 0.15 L. Obtained by ^aHPLC, ^bGC–MS and ^cLC–MS systems.

Further reaction of these species with hydroxyl radicals has led to the formation of corresponding aminophenols, dihydroxybenzenes and carbonic acid monoisopropyl ester. The formation of aminophenols during photocatalytic oxidation of propham was also reported by Muneer et al. (2005) and Bahnemann et al. (2007). However, they were not identified in our work because they are very unstable and rapidly converted to hydroquinone and catechol. In addition, their conversion directly to short-chain carboxylic acids such as maleic, glyoxylic, formic and oxamic acids is also possible. In the second route, the mineralization started with breaking of the C–N bond to form aniline and carbonic acid monoisopropyl ester. The formed aniline was rapidly converted to benzoquinone and further reaction of the latter forms the short-chain carboxylic acids such as maleic, fumaric, glyoxylic and formic acids. The formed by-product carbonic acid monoisopropyl ester was converted to isopropyl alcohol and carbon dioxide. Further oxidation of isopropyl alcohol gives lactic acid, which was not detected in this study; after

that this substance was converted to acetic acid (Flox et al., 2006) and finally to oxalic acid. The nitrogen atoms present in the different structures were released as ammonium and/or nitrate ions. The last stage in the mineralization procedure consisted of conversion of the ultimate carboxylic acids to carbon dioxide and water and thus the total mineralization can be achieved.

4. Conclusions

The electrochemical oxidation of propham has been deeply investigated by using the anodic oxidation process with BDD anode. This electrode behaves as a hydroxyl radical generator under controlled conditions as a result of the water decomposition on the electrode surface. Being a very reactive species and having a very high oxidation power, these radicals ensure the mineralization of propham in aqueous medium. The operational system parameters were optimized.

- Buxton, G.V., Greenstock, C.L., Helman, W.P., Ross, A.B., 1988. Critical review of rate constants for reactions of hydrated electrons, hydrogen atoms and hydroxyl radicals ($\text{OH}^\bullet/\text{O}^\bullet$) in aqueous solutions. *J. Phys. Chem. Ref. Data* 17, 513–886.
- Canizares, P., Garcia-Gomez, J., Lobato, J., Rodrigo, M.A., 2004. Modelization of wastewater electro-oxidation processes: Part I. General description and application to non-active electrodes. *Ind. Eng. Chem. Res.* 34, 87–94.
- Chen, X., Chen, G., 2006. Anodic oxidation of orange II on Ti/BDD electrode: variable effects. *Sep. Purif. Technol.* 48 (1), 45–49.
- Comminellis, Ch., 1994. Electrocatalysis in the electrochemical conversion/combustion of organic pollutants for waste-water treatment. *Electrochim. Acta* 39, 1857–1862.
- Diagne, M., Oturan, N., Oturan, M.A., 2007. Removal of methyl parathion from water by electrochemically generated Fenton's reagent. *Chemosphere* 66 (5), 841–848.
- Felsot, A.S., Rache, K.D., Hamilton, D.J., 2003. Disposal and degradation of pesticide waste. *Rev. Environ. Contam. Toxicol.* 177, 123–200.
- Flox, C., Garrido, J.A., Rodriguez, R.M., Centellas, F., Cabot, P., Arias, C., Brillas, E., 2005. Degradation of 4,6-dinitro-*o*-cresol from water by anodic oxidation with a boron-doped diamond electrode. *Electrochim. Acta* 50, 3685–3692.
- Flox, C., Cabot, P.L., Centellas, F., Garrido, J.A., Rodríguez, R.M., Arias, C., Brillas, E., 2006. Electrochemical combustion of herbicide mecoprop in aqueous medium using a flow reactor with a boron-doped diamond anode. *Chemosphere* 64, 892–902.
- Guinea, E., Arias, C., Cabot, P.L., Garrido, J.A., Rodríguez, R.M., Centellas, F., Brillas, E., 2008. Mineralization of salicylic acid in acidic aqueous medium by electrochemical advanced oxidation processes using platinum and boron-doped diamond as anode and cathodically generated hydrogen peroxide. *Water Res.* 42 (1–2), 499–511.
- Hanna, K., Chiron, S., Oturan, M.A., 2005. Coupling enhanced water solubilization with cyclodextrin to indirect electrochemical treatment for pentachlorophenol contaminated soil remediation. *Water Res.* 39, 2763–2773.
- Iniesta, J., Gonzalez-Garcia, J., Exposito, E., Montiel, V., Aldaz, A., 2001. Influence of chloride ion on electrochemical degradation of phenol in alkaline medium using bismuth doped and pure PbO_2 anodes. *Water Res.* 35 (14), 3291–3300.
- Kosutic, K., Kunst, B., 2002. Removal of organics from aqueous solutions by commercial RO and NF membranes of characterized porosities. *Desalination* 142, 47–56.
- Lissens, G., Pieters, J., Verhaege, M., Pinoy, L., Verstraete, W., 2003. Electrochemical degradation of surfactants by intermediates of water discharge at carbon-based electrodes. *Electrochim. Acta* 48 (12), 1655–1663.
- Malpass, G.R.P., Miwa, D.W., Machado, S.A.S., Motheo, A.J., 2006. Oxidation of the pesticide atrazine at DSAs electrodes. *J. Hazard. Mater. B* 137, 565–572.
- Marselli, B., Garcia-Gomez, J., Michaud, P.A., Rodrigo, M.A., Comminellis, Ch., 2003. Electrogeneration of hydroxyl radicals on boron-doped diamond electrodes. *J. Electrochem. Soc.* 150, D79–D83.
- Martinez-Huitle, C.A., Ferro, S., De Battisti, A., 2005. Electrochemical incineration in the presence of halides. *Electrochem. Solid-State Lett.* 11, D35–D39.
- Michaud, P.A., Panizza, M., Ouattara, L., Diaco, T., Foti, G., Comminellis, Ch., 2003. Electrochemical oxidation of water on synthetic boron-doped diamond thin film anodes. *J. Appl. Electrochem.* 33, 151–154.
- Mitadera, A., Spataru, N., Fujishima, A., 2004. Electrochemical oxidation of aniline at boron-doped diamond electrodes. *J. Appl. Electrochem.* 34, 249–254.
- Muneer, M., Qamar, M., Saquib, M., Bahnemann, D.W., 2005. Heterogeneous photocatalysed reaction of three selected pesticide derivatives, protham, propachlor and tebuthiuron in aqueous suspensions of titanium dioxide. *Chemosphere* 61, 457–468.
- Muruganathan, M., Yoshihara, S., Rakuma, T., Uehara, N., Shirakashi, T., 2007. Electrochemical degradation of 17 β -estradiol (E2) at boron-doped diamond (Si/BDD) thin film electrode. *Electrochim. Acta* 52 (9), 3242–3249.
- Neyens, E., Bayeans, J., 2003. A review of the classic Fenton's peroxidation as an advanced oxidation technique. *J. Hazard. Mater.* 98 (1–3), 33–50.
- Orejuela, E., Silva, M., 2004. Determination of protham and chlorprotham in postharvest-treated potatoes by liquid chromatography with peroxyoxalate chemiluminescence detection. *Anal. Lett.* 37, 2531–2543.
- Oturan, M.A., 2000. An ecologically effective water treatment technique using electrochemically generated hydroxyl radicals for in situ destruction of organic pollutants. *J. Appl. Electrochem.* 30, 475–482.
- Oturan, M.A., Oturan, N., Lahite, C., Trévin, S., 2001. Production of hydroxyl radicals by electrochemically assisted Fenton's reagent. Application to the mineralization of an organic micro-pollutant, pentachlorophenol. *J. Electroanal. Chem.* 507, 96–102.
- Ozcan, A., Sahin, Y., Kopal, A.S., Oturan, M.A., 2007. Degradation of picloram by the electro-Fenton process. *J. Hazard. Mater.*, in press.
- Oturan, M.A., Brillas, E., 2007. Electrochemical advanced oxidation processes (EAOPs) for environmental applications. *Port. Electrochim. Acta* 25, 1–18.
- Panizza, M., Cerisola, G., 2005. Application of diamond electrodes to electrochemical processes. *Electrochim. Acta* 51, 191–199.
- Pignatello, J.J., Oliveros, E., MacKay, A., 2006. Advanced oxidation processes for organic contaminant destruction based on the Fenton reaction and related chemistry. *Crit. Rev. Environ. Sci. Technol.* 36, 1–84.
- Polcaro, A.M., Vacca, A., Mascia, M., Palmas, S., 2005. Oxidation at boron doped diamond electrodes: an effective method to mineralise triazines. *Electrochim. Acta* 50, 1841–1847.
- Rodrigo, M.A., Michaud, P.A., Duo, I., Panizza, M., Cerisola, G., Comminellis, Ch., 2001. Oxidation of 4-chlorophenol at boron-doped diamond electrodes for wastewater treatment. *J. Electrochem. Soc.* 148, D60–D64.
- Scialdone, O., Galia, A., Guarisco, C., Randazzo, S., Filardo, G., 2007. Electrochemical incineration of oxalic acid at boron doped diamond anodes: role of operative parameters. *Electrochim. Acta*, in press.
- Sharifian, H., Kirk, D.W., 1986. Electrochemical oxidation of phenol. *J. Electrochem. Soc.* 133, 921–924.
- Simond, O., Schaller, V., Comminellis, Ch., 1997. Theoretical model for the anodic oxidation of organics on metal oxide electrodes. *Electrochim. Acta* 42, 2009–2012.
- Sirés, I., Centellas, F., Garrido, J.A., Rodríguez, R.M., Arias, C., Cabot, P.L., Brillas, E., 2007. Mineralization of clofibric acid by electrochemical advanced oxidation processes using a boron-doped diamond anode and Fe^{2+} and UVA light as catalysts. *Appl. Catal. B: Environ.* 72, 373–381.
- Tatapudi, P., Fenton, J.M., 1994. Electrolytic processes for pollution treatment and pollution prevention. In: Gerischer, H. (Ed.), *Advances in Electrochemical Engineering*. VCH, Weinheim, pp. 363–417.
- Un, U.T., Altay, U., Kopal, A.S., Ogutveren, U.B., 2007. Complete treatment of olive mill wastewaters by electrooxidation. *Chem. Eng. J.*, in press.
- Vlyssides, A., Barampouti, E.M., Mai, S., Arapoglou, D., Kotronarou, A., 2004. Degradation of methylparathion in aqueous solution by electrochemical oxidation. *Environ. Sci. Technol.* 38, 6125–6131.
- World Health Organization Technical Report, 2001. *Chemistry and Specifications of Pesticides*, vol. 899, Geneva.